

Model of silica glass from combined classical and *ab initio* molecular–dynamics simulations

M. Benoit^a, S. Ispas, P. Jund, and R. Jullien

Laboratoire des Verres, Université Montpellier II, cc 69, Place E. Bataillon, 34095 Montpellier, France

Received 23 March 1999 and Received in final form 15 July 1999

Abstract. A Car-Parrinello (CP) molecular dynamics simulation of vitreous silica, combined with classical molecular dynamics, is presented. The equilibration of the liquid, quench and relaxation of the glass are performed classically using the van Beest, Kramer and van Santen (BKS) potential [12] and the resulting configuration (coordinates and velocities) is used as input for the CP simulation. A remarkable stability of the CP dynamics is observed justifying this procedure and validating the BKS potential. Several structural and electronic properties are calculated and compared with experiments.

PACS. 61.43.Fs Glasses – 71.15.Pd Molecular dynamics calculations (Car-Parrinello) and other numerical simulations – 61.43.Bn Structural modeling: serial-addition models, computer simulation

1 Introduction

Silica is a common material that plays a key role in the glass manufacturing industry as well as in electronic devices. It is also of great importance in chemistry and geology as a network forming glass [1]. In the past twenty years, numerical simulations have been extensively used in order to investigate the structural and vibrational properties of amorphous silica [2–5] which are still largely misunderstood. For example the origin of the medium-range order, of the so-called boson peak and of the two defect lines in the Raman spectrum is still controversial [6–9]. However molecular dynamics (MD) simulations have improved our understanding of the microscopic structure of amorphous silica and the development of interaction potential based on *ab initio* parameters have produced results in good agreement with experimental data [3].

More recently, with the development of parallel computers, the study of disordered silica within the framework of *ab initio* calculations has become accessible [10]. The explicit treatment of the electronic structure has permitted to improve the description of the structure and in the same time to give access to the electronic properties of disordered SiO₂. But first-principles approaches to the study of disordered systems can not be carried out without encountering several difficulties. The major one is due to the limited size of the system that can be treated with *ab initio* calculations. Secondly the dynamics is very costly: the maximum length of the trajectory that can be calculated within the framework of the Car-Parrinello (CP) method [11] is of the order of ten picoseconds, which

is far from the typical relaxation times of disordered systems.

In order to partially prevent these difficulties, we have performed a Car-Parrinello molecular dynamics simulation of vitreous SiO₂ combined with a classical molecular dynamics simulation using the van Beest *et al.* interaction potential [12]. In this novel approach, the silica glass is obtained by equilibrating the silica liquid and quenching it to 300 K using the classical MD method. The glass thus obtained is first equilibrated with the classical potential and then equilibrated using the Car-Parrinello method. The study of the vitreous SiO₂ system with first-principles is thus accessible at a much lower CPU time cost since the equilibration of the liquid, the quench and a part of the relaxation are carried out within the framework of classical molecular dynamics. The second section of this paper describes the model and gives the details of the simulations. In the third section, we present structural and electronic characteristics of our glass sample and compare them to experimental values when possible. The last section is a conclusion part.

2 Model

We began by performing classical molecular dynamics simulations for a microcanonical system containing 216 silicon atoms and 432 oxygen atoms confined in a cubic box of edge length 21.48 Å which corresponds to a mass density of ≈ 2.18 g/cm³, with periodic boundary conditions. The interaction potential is the so-called BKS potential developed by van Beest *et al.* [12]; some aspects of similar simulations are reported in reference [13]. A time step of 0.7 fs was used. A liquid sample was generated by melting

^a e-mail: magali@ldv.univ-montp2.fr

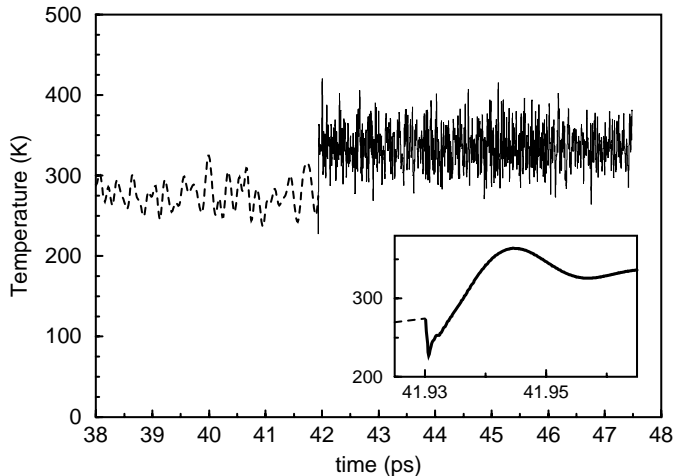


Fig. 1. Evolution of the temperature of the ions as a function of the simulation time in picoseconds. The end of the classical MD trajectory is shown in dashed line, the full CP trajectory is shown in solid line. In the inset, a zoom of the beginning of the CP trajectory is depicted.

a β -cristobalite crystal at a temperature around 5000 K, from which we have extracted a cubic box of edge length 10.558 Å containing 26 silicon atoms and 52 oxygen atoms. This new liquid sample, of a mass density of $\approx 2.2 \text{ g/cm}^3$, was then fully equilibrated during $\approx 35 \text{ ps}$ and used as the initial configuration for the quench. The system was cooled to 300 K at a quench rate of $5 \times 10^{13} \text{ K/s}$ which was obtained by removing the corresponding amount of energy from the total energy of the system at each iteration. Although the glass transition temperature is abnormally high ($T_g \approx 3000 \text{ K}$) compared to experiments, due to the too high cooling rate, the structural [3,13], dynamical [4] and thermal [14] properties of the resulting glass fit well with experiments.

The obtained glass was relaxed during $\approx 40 \text{ ps}$ and then it was used as the initial configuration for the Car-Parrinello simulation performed with the CPMD code developed in Stuttgart [15]. We report in Figure 1 the evolution of the ionic temperature as a function of the simulation time for the end of the classical MD trajectory and the full CP trajectory. One can notice that, after a small heating up of the ions, the system remains remarkably stable. In the CP simulation, after a short relaxation (see inset of Fig. 1), the temperature equilibrates around an average value of $\approx 335 \text{ K}$, which is approximately 50 K higher than the average classical MD temperature ($\approx 281 \text{ K}$). This temperature jump is unexpectedly small if one considers the strong differences between the two descriptions.

The glass was equilibrated during 0.7 ps and data were accumulated on the following 5.0 ps. In the CP simulation the electronic structure was described within the density functional theory (DFT) in the local density approximation (LDA) [17]. We adopted a plane wave pseudopotential approach using conventional pseudopotentials for silicon [16] and oxygen [18]. The electronic wavefunctions were expanded at the Γ point of the supercell on a plane waves basis set up to an energy cutoff of 70 Ry, at which

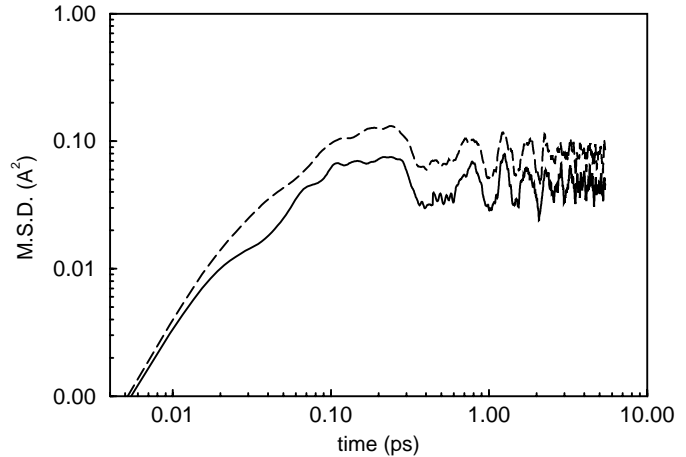


Fig. 2. Mean square displacements of silicon atoms (solid line) and oxygen atoms (long-dashed line) at 300 K as a function of the simulation time in picoseconds.

good convergence in the structural properties was achieved at 0 K in cristobalite and α -quartz. A time step of 5 a.u. (0.12 fs) and a fictitious electronic mass of 600 a.u. were used to integrate the equations of motion.

3 SiO₂ structural and electronic properties

In order to check the structure of the generated glass, we have analyzed several structural characteristics of the sample and compared them to experiments when possible. These structural characteristics have also been compared to the ones obtained from the continuation of the classical molecular dynamics simulation using the BKS potential, starting from the same initial configuration as the CP simulation. Then we have analyzed the electronic properties of the CP sample.

At 300 K, the mean square displacements (MSD) of the atoms show a strong overshoot around 0.25 ps and then no diffusion after the first 0.5 ps (see Fig. 2). Then they oscillate around 0.047 Å^2 for silicon atoms and around 0.080 Å^2 for oxygen atoms with a period roughly equal to 0.5 ps. The overshoot and the oscillations are known to be related to the boson peak observed by Raman spectroscopy and inelastic neutron scattering [5]. The amplitude of these oscillations ($\approx 0.02 \text{ Å}^2$) is too high when compared to recent results of molecular dynamics simulations on systems containing 256 SiO₂ units [5]. In these simulations, the MSD of silicon atoms oscillates around 0.04 Å^2 and the one of oxygen atoms around 0.06 Å^2 , the amplitude of these oscillations being less than 0.005 Å^2 . This discrepancy is essentially due to our limited system size. However the time evolution of the MSD is in very good agreement with the results reported in reference [5].

At this stage, it is interesting to examine how much the structure of the *ab initio* glass differs from that of the BKS glass used as the starting configuration. In Figure 3 we show the evolution of the mean values of the Si–O–Si and O–Si–O angle distributions as a function of

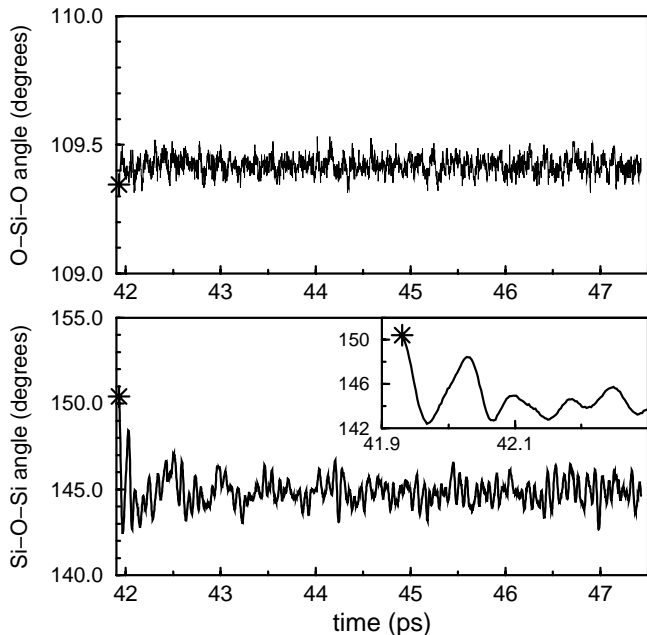


Fig. 3. Evolution of the mean values of the angle distributions as a function of the simulation time. Upper graph: O-Si-O angles. Lower graph: Si-O-Si angles. The stars denote the mean values of the angles distribution in the classical starting configuration.

the simulation time of the CP trajectory. The stars indicate the mean value of these distributions for the initial classical configuration. If the tetrahedral angles stay very close to the exact value of $109^\circ 4$ in both descriptions (BKS and CP), the inter-tetrahedral angles are quite different. As soon as the Car-Parrinello simulation is started, the mean value of the Si-O-Si angle distribution decreases from 150° to 145° , both values lying in the error bars of the experimental angle (140 - 150°) [19]. This decrease is shown in the inset of the lower graph of Figure 3 and one can notice that the rearrangement of the structure occurs on very short period of times (≈ 0.2 ps) which can be related to the stabilisation time of the temperature in the CP trajectory (see Fig. 1).

We have equally evaluated the time-averaged distributions of the two angles O-Si-O and Si-O-Si (see Fig. 4) and compared them to the time-averaged distributions obtained by continuing the classical MD simulation over ≈ 42 ps from the same starting configuration as the CP dynamics. As one can notice, the main differences between the CP and the BKS angle distributions reside in a shift of the Si-O-Si distribution towards lower values of the angle. This shift reflects the decrease of the mean angle observed at the beginning of the CP trajectory. There is also a splitting of the Si-O-Si distribution in the BKS case which is not present in the CP one. This splitting is probably an artefact due to the small system simulation, since it is not observed in larger systems [13]. In the CP simulation, the first moments of the angle distributions give averaged values of $145^\circ \pm 13$ for Si-O-Si angles and of $109^\circ \pm 7$ for O-Si-O angles, values closer to experimental values than those obtained by Pasquarello *et al.* for the inter-tetrahedral angles ($136^\circ \pm 14$) [10], which may

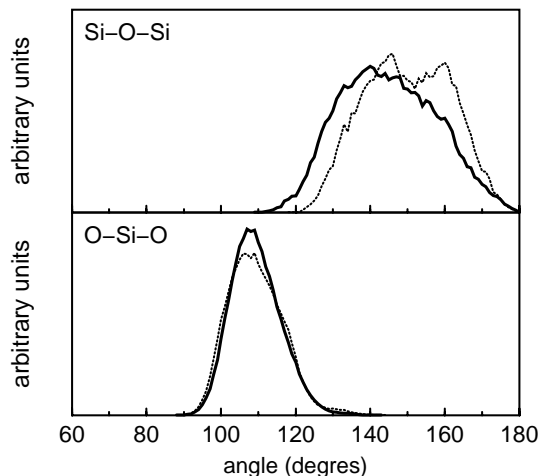


Fig. 4. Averaged angle distributions: intertetrahedral Si-O-Si (upper graph) and intratetrahedral O-Si-O (lower graph). Solid lines are Car-Parrinello MD distributions and dotted lines are classical MD distributions.

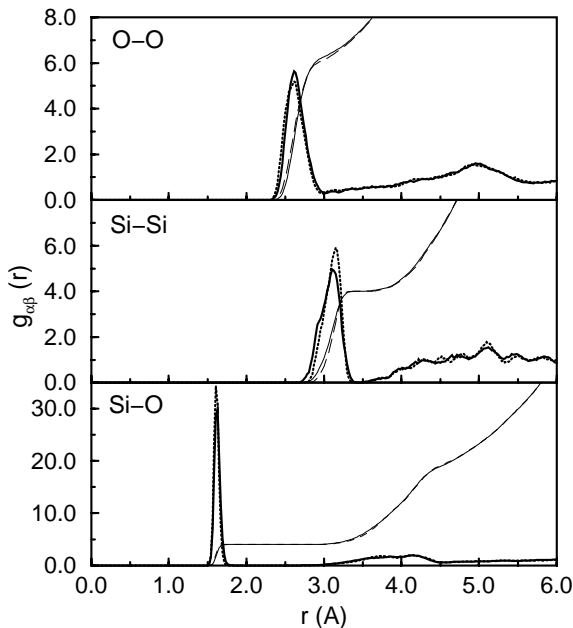


Fig. 5. Pair correlation functions $g_{\alpha\beta}(r)$ for O-O (upper graph), Si-Si (middle graph) and Si-O (lower graph). Solid and dotted lines are the pair correlation functions obtained from the Car-Parrinello MD simulation and from the classical MD simulation, respectively. The thin solid lines and the long dashed lines are the corresponding integrated coordination numbers, respectively.

be due to the use of a different sample density, or to a different cooling rate. For our amorphous sample, we have checked the density by computing the total energy as a function of the volume at $T = 0$ K. We have found that a minimum energy is obtained for a density of 2.23 g/cm³, which is slightly higher than the chosen initial value but still very close to the experimental density.

As a second structural characteristic, we have calculated the pair correlation functions $g_{\alpha\beta}(r)$ ($\alpha, \beta = \text{Si, O}$) of glassy SiO₂. One can notice that the two descriptions give very similar results (see Fig. 5). Only the Si-Si first

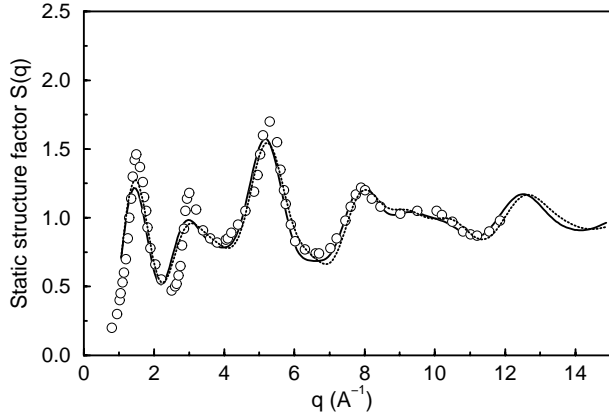


Fig. 6. Comparison between simulated $S(q)$ as defined in equation (1), computed from the CP simulation (solid line), experimental neutron $S(q)$ from reference [21] (circles) and computed from the classical MD simulation (dotted line).

peak seems to be slightly shifted towards lower values of r in the CP description which is consistent with the shift of the Si–O–Si angle distribution (see Fig. 3). In the CP simulation, the average first neighbour Si–O distance is equal to 1.62 Å, the O–O distance to 2.66 Å and the Si–Si distance to 3.08 Å, which show very good agreement with experimental values [20]. The coordination of the silicon atoms is equal to 4, which reflects a perfect tetrahedral arrangement. We have compared our pair correlation functions to those found in recent *ab initio* molecular dynamics simulations [10] and they are overall similar.

Finally, only the Si–O–Si angles and the Si–Si distances change in the Car-Parrinello dynamics compared to the classical BKS dynamics. These changes can not be attributed to the temperature (the difference is too small) and might be explained by the fact that no Si–Si short-range attraction term is included in the BKS potential, therefore leading to an increase of the Si–O–Si angle and of the Si–Si distance, with respect to the DFT description.

Further, these structural results can be compared directly to experiments by calculating the static structure factor as obtained from neutron diffraction. The static structure factor was computed using the following formulae:

$$S(q) = 1 + 4\pi \frac{N}{V} \int_0^{r_{\max}} (g(r) - 1) \frac{\sin(qr)}{qr} r^2 dr \quad (1)$$

where

$$g(r) = \frac{\left[\sum_{\alpha, \beta} c_{\alpha} b_{\alpha} c_{\beta} b_{\beta} g_{\alpha\beta}(r) \right]}{\left[\sum_{\alpha} c_{\alpha} b_{\alpha} \right]^2}. \quad (2)$$

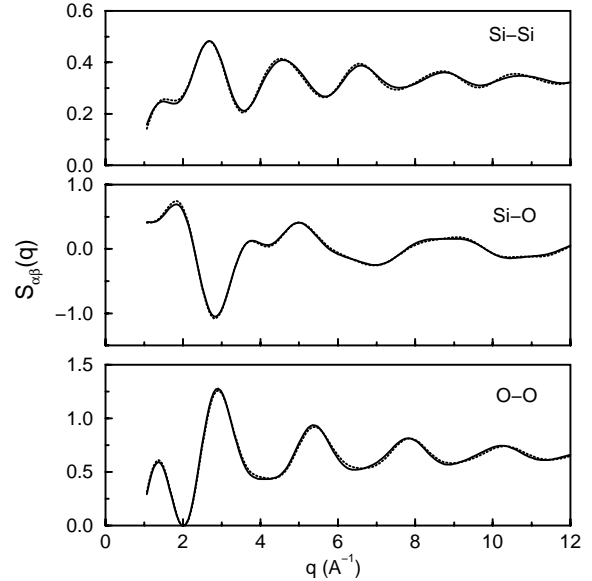


Fig. 7. Partial structure factors $S_{\alpha\beta}(q)$ for Si–Si (upper graph), Si–O (middle graph) and O–O (lower graph). Solid lines denote the CP results and dotted lines the classical MD ones.

In the above equations, $r_{\max} = L/2$ where L is the edge of the box, the $g_{\alpha\beta}(r)$ are the pair correlation functions ($\alpha, \beta = \text{Si, O}$), c_{α} and c_{β} are the concentrations of the two species and b_{α} and b_{β} are their scattering lengths taken equal to 4.149 fm for Si and to 5.803 fm for O [21]. In Figure 6, we show the static structure factor computed using the above definition and compare it to experimental data (circles) obtained from neutron scattering experiments [21], and to the classical MD one. One may notice that the agreement between our results and experimental ones is very good for large values of q and still quite good for small q concerning the maxima and minima positions. However the amplitudes of the first and second peaks are slightly too small compared to experiment, which is due to our limited system size. The comparison with the BKS structure factor is also quite good, but some slight discrepancies appear at large values of q which may be related to the Si–Si correlations. In the CP structure factor, the first sharp diffraction peak (FSDP) appears at $q \approx 1.48 \text{ \AA}^{-1}$ which is to be compared with the experimental value of 1.52 \AA^{-1} [21].

The origin of the peaks in the total neutron structure factor can be inferred from partial structure factors as depicted in Figure 7. These partial structure factors $S_{\alpha\beta}$ are computed from the pair correlation functions $g_{\alpha\beta}(r)$. The FSDP seems to be a result of the combination of Si–Si, Si–O and O–O correlations. While the second peak clearly involves contributions from the Si–Si and O–O correlations, the third and fourth peaks consist of Si–O, Si–Si and O–O correlations. As one can notice, the BKS and CP simulations give very similar partial structure factors that are hardly distinguishable. Only very small differences can be noted in the peak positions of the Si–Si and the O–O

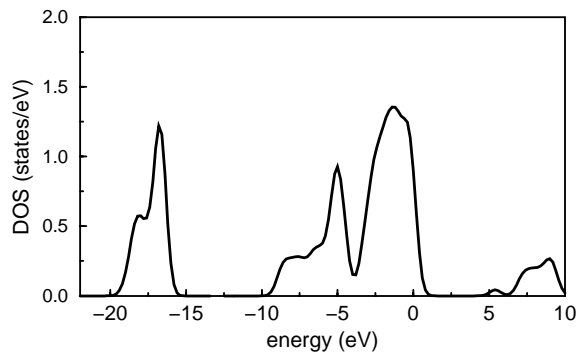


Fig. 8. Electronic density of states of the glass sample at ≈ 5 ps. The curve was smoothed with a Gaussian broadening.

ones at large values of q , that can be related to the Si-Si distance and the Si-O-Si angle changes.

The electronic properties of the CP silica glass were analyzed in terms of the electronic density of states. We selected a given configuration of the glass sample at the end of the CP trajectory and computed the Kohn-Sham density of states (see Fig. 8). The density agrees well with other DFT calculations [10] and gives a band gap of 5.0 eV (to be compared to 4.8 eV [10]) but underestimates the experimental value (~ 9 eV). On the opposite, Kowalski *et al.* [22] computed the electronic density of states using a tight-binding Hamiltonian, on ionic configuration of α -SiO₂ generated by molecular dynamics, and obtained a better estimate of the band gap (≈ 9 eV). This discrepancy is usual in DFT calculations [23]. However the different states are well reproduced and correspond to oxygen $2s$ states at about -20 eV, to bonding states between Si sp^3 hybrids and O $2p$ orbitals (from -10 to -4 eV), to O $2p$ nonbonding orbitals for the highest occupied states and to antibonding orbitals for the lowest conduction band.

4 Conclusion

Using a combination of classical and *ab initio* molecular dynamics simulations, we have studied structural and electronic properties of a silica glass. The originality of this work resides in the preparation of the glass sample: using classical MD, a silica glass was generated and taken as the initial configuration of a first-principles MD simulation. The remarkable stability of the Car-Parrinello simulation compared to the classical trajectory (temperature and diffusion) validates this method and our choice of the classical potential. Moreover, this method allows to study the glass sample by means of *ab initio* molecular dynamics saving the time of the equilibration of the liquid and of the quench. The possible trapping into a local minimum of the classical potential was investigated. Another classical sample was used as an input for the CP molecular dynam-

ics simulation and gave very similar structural properties. Further checks are being performed [24].

The structural properties of the obtained glass were analyzed in terms of pair correlations functions, angle distributions and structure factor. The electronic density of states was also calculated. Both structural and electronic characteristics are in good agreement with former *ab initio* calculations and experiments. By comparing the structural characteristics of the BKS and CP simulations, we show that only the Si-Si distances and the Si-O-Si angles are slightly different although they all lie inside the experimental error bars. These differences might be attributed to the lack of the Si-Si short-range attraction term in the BKS potential.

In conclusion, we have generated a model of glassy SiO₂ which presents satisfying structural and electronic properties, by using a novel preparation method that allows a considerable time saving. This *ab initio* glass sample will then be used for accurate studies of vitreous silica in presence of defects or impurities. This approach could also be generalized to other simple glassy materials for which good classical potentials are available, giving access to their accurate local structure and to their electronic properties, at finite temperature.

M. Benoit would like to thank D. Marx, M. Tuckerman, J. Hutter and M. Parrinello for helpful discussions and support. Calculations have been performed on the CRAY/T3E at the I.D.R.I.S. computer center in Orsay (France) and on the IBM/SP2 at the C.N.U.S.C. computer center in Montpellier (France).

References

1. *The Physics and Technology of Amorphous SiO₂*, edited by R.A.B. Devine (Plenum Press, New York, 1988).
2. R.G. Della Valle, H.C. Andersen, J. Chem. Phys. **97**, 2682 (1992); A. Nakano, L. Bi, R.K. Kalia, P. Vashishta, Phys. Rev. Lett. **71**, 85 (1993); W. Jin, R.K. Kalia, P. Vashishta, Phys. Rev. B **50**, 118 (1994).
3. K. Vollmayr, W. Kob, K. Binder, Phys. Rev. B **54**, 15808 (1996).
4. S.N. Taraskin, S.R. Elliott, Europhys. Lett. **39**, 37 (1997).
5. B. Guillot, Y. Guissani, Phys. Rev. Lett. **78**, 2401 (1997).
6. S.R. Elliott, Phys. Rev. Lett. **67**, 711 (1991).
7. R.A. Barrio, F.L. Galeener, E. Martinez, R.J. Elliott, Phys. Rev. B **48**, 15672 (1993).
8. P.H. Gaskell, D.J. Wallis, Phys. Rev. Lett. **76**, 66 (1996).
9. F.J. Bermejo, A. Criado, J.L. Martinez, Phys. Lett. A **195**, 236 (1994).
10. J. Sarnthein, A. Pasquarello, R. Car, Phys. Rev. Lett. **74**, 4682 (1995); J. Sarnthein, A. Pasquarello, R. Car, Phys. Rev. B **52**, 12 690 (1995); A. Pasquarello, J. Sarnthein, R. Car, Phys. Rev. B **57**, 14133 (1998); M. Boero, A. Pasquarello, J. Sarnthein, R. Car, Phys. Rev. Lett. **78**, 887 (1997).

11. R. Car, M. Parrinello, Phys. Rev. Lett. **55**, 2471 (1985).
12. B.W.H. van Beest, G.J. Kramer, R.A. van Santen, Phys. Rev. Lett. **64**, 1955 (1990).
13. P. Jund, R. Jullien, Phil. Mag. A **79**, 223 (1999).
14. P. Jund, R. Jullien, Phys. Rev. B **59**, 13707 (1999).
15. CPMD Version 3.0, J. Hutter, P. Ballone, M. Bernasconi, P. Focher, E. Fois, St. Goedecker, M. Parrinello, M. Tuckerman, MPI für Festkörperforschung and IBM Research 1990-96.
16. G.B. Bachelet, D.R. Haman, M. Schlüter, Phys. Rev. B **26**, 4199 (1982).
17. W. Kohn, L. Sham, Phys. Rev. A **140**, 1133 (1965).
18. N. Trouiller, J.L. Martins, Phys. Rev. B **43**, 1993 (1991).
19. R. Dupree, R.F. Pettifer, Nature **308**, 523 (1991).
20. P.A.V. Johnson, A.C. Wright, R.N. Sinclair, J. Non-Cryst. Solids **58**, 109 (1983).
21. S. Susman, K.J. Volin, D.L. Price, M. Grimsditch, J.P. Rino, R.K. Kalia, P. Vashishta, G. Gwanmesia, Y. Wang, R.C. Liebermann, Phys. Rev. B **43**, 1194 (1991).
22. T. Kowalski, W. Kob, K. Vollmayr, Phys. Rev. B **56**, 9469 (1997).
23. R.W. Godby, M. Schlüter, L.J. Sham, Phys. Rev. B **37**, 10 159 (1988).
24. S. Ispas, M. Benoit, P. Jund, R. Jullien (in preparation).